

Inhibition of the Corrosion of Iron by Oxygen and Nitrogen Containing Compounds

K. K. Al-Neami¹, A. K. Mohamed², I. M. Kenawy², A. S. Fouda^{2,*}

¹ Chemistry Department, Faculty of Science, Qatar University, Qatar-Doha, P.O. Box 2713

² Chemistry Department, Faculty of Science, Mansoura University, Mansoura, Egypt

Summary. Corrosion inhibition by quinine, ephedrine, brucine, cinchonine, codeine, and harmaline with respect to the dissolution of iron in 2 M sulphuric acid was measured using electrochemical methods. Polarization curves indicated that these compounds act as mixed-type inhibitors, *i.e.* both the cathodic and anodic curves are affected. The observed effect follows the *Temkin* adsorption isotherm. The effect of the different structural features of these compounds on their inhibition efficiency has been studied. Results indicate that the rate of corrosion of iron increases with increasing temperature over the range 30–50 °C both in the absence and in the presence of inhibitors. Some thermodynamic functions were also computed and are discussed.

Keywords. Acid corrosion; Inhibition; Iron; Oxygen and nitrogen containing compounds.

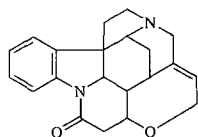
Korrosionshemmung bei Eisen durch Sauerstoff- und Stickstoffverbindungen

Zusammenfassung. Die von Chinin, Ephedrin, Brucin, Chinchonin, Codein und Harmalin ausgeübte Korrosionshemmung bei der Auflösung von Eisen in 2 M Schwefelsäure wurde mittels elektrochemischer Methoden untersucht. Polarisationskurven zeigen, daß die erwähnten Verbindungen als Inhibitoren gemischten Typs fungieren, d. h. sowohl die kathodische als auch die anodische Kurve wurde beeinflußt. Der beobachtete Effekt folgt der *Temkinschen* Adsorptionsisotherme. Die Auswirkung von Strukturänderungen auf die Effizienz der Hemmung und einige thermodynamische Funktionen werden diskutiert. Die Korrosionsrate von Eisen steigt sowohl in Gegenwart als auch in Abwesenheit der Inhibitoren im Bereich von 30–50 °C mit steigender Temperatur.

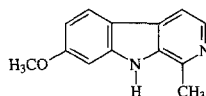
Introduction

Corrosion inhibition efficiency strongly depends on the structure and chemical properties of the layers formed at the surface of the metal under particular experimental conditions. In the case of the heterocyclic nitrogen compounds under investigation in acidic media, the adsorption is ascribed to effects connected with the aromatic rings. It has been reported that the adsorption of heterocyclic compounds occurs with the aromatic rings parallel to the metal surface [1]. The adsorption appears to depend mainly on the electronic structure of the molecules and the inhibition efficiency increases with the length of the hydrocarbon chain and

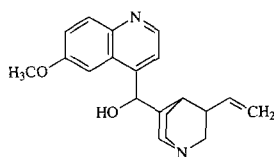
the number of aromatic rings [2–6]. The present study has been performed in order to deduce the mechanism of the inhibition exerted by these compounds and the effect of structural changes on their inhibition efficiency. The selection of the compounds has been due mainly to their high molecular weights and also to their anaesthetic effect.



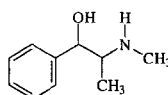
Brucine



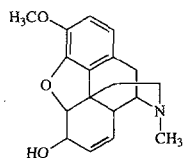
Harmaline



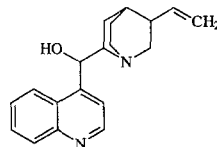
Quinine



Ephedrine



Codeine



Chinchonine

Results and Discussion

Figure 1 shows the anodic and cathodic *Tafel* plots of iron in the presence of different concentrations of brucine. For comparison, polarization curves measured in 2 M sulphuric acid solution are also plotted. These compounds induce an increase in both the cathodic and anodic overvoltages and cause a parallel displacement of both the cathodic and the anodic *Tafel* curves. The results indicate that the presence of these compounds in the solution inhibits both the hydrogen evolution and the anodic dissolution processes. The data suggest that these compounds act as mixed-type inhibitors. They also indicate that the molecules of these substances are mainly adsorbed at the surface of the iron *via* the oxygen and nitrogen centers of adsorption. The corrosion current density, i_{corr} , for iron in 2 M sulphuric acid is $21.88 \text{ mA}\cdot\text{cm}^{-2}$. Addition of the compounds tested induces a decrease in i_{corr} this indicates that these compounds act as inhibitors for iron dissolution in sulphuric acid.

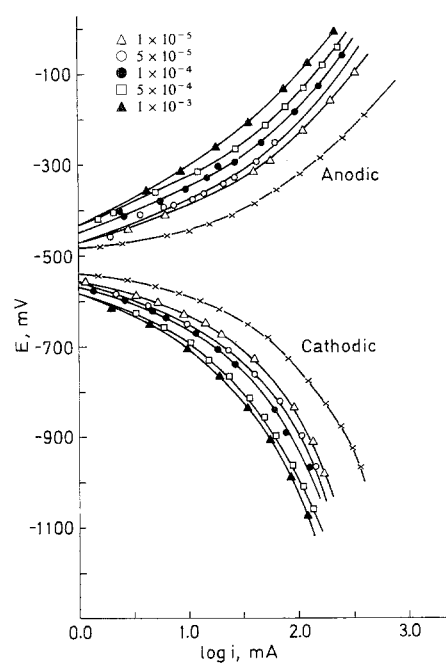


Fig. 1. Polarization curves for iron in 2 M H_2SO_4 containing various concentrations of brucine

Table 1 gives the effect of concentration of brucine on i_{corr} , anodic and cathodic Tafel slopes, E_{corr}^0 , and percentage inhibition efficiency. It can be seen from Table 1 that, as the concentration increases, the value of i_{corr} decreases and hence the percentage inhibition efficiency increases. This indicates that the inhibition efficiency depends on the concentration of the inhibitors. In the presence of the inhibitors, the open-circuit potential was shifted to the negative side. When an external *emf* was applied, both the cathode and the anode were polarized due to the presence of the nitrogen atom which is responsible for the cathodic behaviour and the oxygen atom which is responsible for the anodic behaviour. Similar behaviour was observed in the presence of different additives. The data show that the slopes of the cathodic and anodic Tafel lines (B_c and B_a) remain almost unchanged on increasing the concentration of the tested compounds and have the values $B_c = 0.225$ – 0.210 and

Table 1. The effect of brucine concentration on the free corrosion potential, Tafel slopes, corrosion current density, and percentage inhibition of corrosion of iron in 2 M sulphuric acid at $30 \pm 1^\circ C$

Conc. (M)	$-E_{\text{corr}}$ (mV/decade)	i_{corr} (mA/cm ²)	β_c (V/decade)	β_a (V/decade)	% Inhibition
0.00	455	21.88	0.225	0.150	—
1×10^{-5}	450	8.10	0.220	0.140	63.0
5×10^{-5}	445	7.60	0.220	0.140	65.3
1×10^{-4}	442	6.60	0.210	0.135	69.8
5×10^{-4}	440	6.00	0.210	0.135	72.5
1×10^{-3}	437	5.50	0.210	0.135	74.9

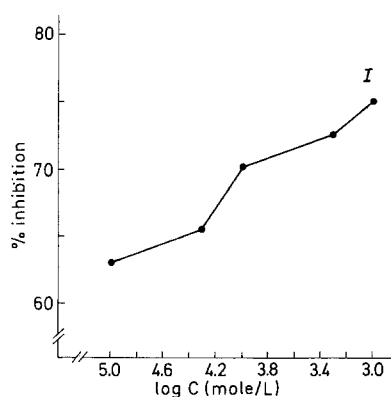


Fig. 2. Effect of the concentration of brucine on the inhibition

Table 2. Effect of inhibitor efficiency on percentage inhibition in acidic solution at 30 °C using polarization measurements

Conc. (M)	% Inhibition					
	a	b	c	d	e	f
1×10^{-5}	63.0	52.2	40.0	31.2	25.1	23.4
5×10^{-5}	65.3	54.3	42.5	33.9	27.6	25.6
1×10^{-4}	69.8	66.9	65.3	54.3	45.1	40.5
5×10^{-4}	72.5	71.2	68.4	63.7	60.2	56.3
1×10^{-3}	74.9	72.5	71.2	68.4	69.8	65.5

a = brucine, b = quinine, c = codeine, d = cinchonine, e = harmaline, f = ephedrine

$B_a = 0.15-0.135$ V/decade. This behaviour indicates that the adsorbed compounds mechanically screen the coated part of the electrode and therefore protect it from the action of the corrosive medium. These molecules have no effect on the mechanism of the dissolution of iron but cause only inactivation of a part of the surface with respect to the corrosive medium. A plot of % inhibition vs. $\log C$ (Fig. 2) of brucine has the character of an s-shaped adsorption isotherm.

It is evident from Table 2 and Fig. 3 (shows the polarizarion curves of iron in the presence of 5×10^{-5} M of different additives used) that the order of increasing inhibition efficiency of the tested compounds in 2 M sulphuric acid is brucine > quinine > codeine > cinchonine > harmaline > ephedrine.

A correlation between θ and $\log C$ of adsorbate is given by the *Temkin* adsorption isotherm. The experimental results (Fig. 4) are in good agreement with the following equations 6 and 7 showing that the adsorption of the additives used follow the *Temkin* adsorption isotherm.

$$\theta = \text{cons} + (2.303/f) \cdot \log C \quad 6$$

$$f = (1/RT) \cdot d(\Delta G^\#)/d\theta \quad 7$$

The inhibition efficiency of additives depends on many factors which include the number of adsorption sites and their charge density, molecular size and mode of

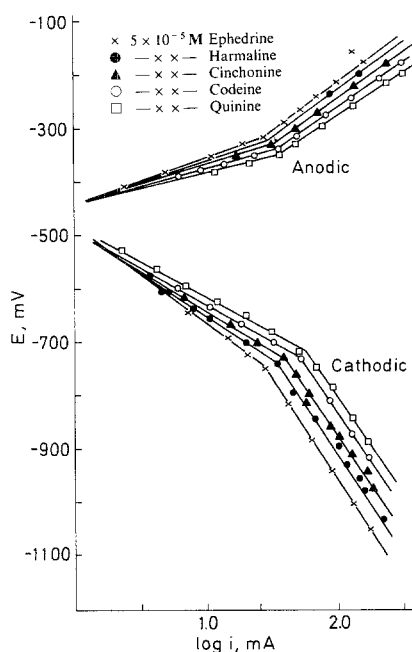


Fig. 3. Polarization curves for iron in $2\text{ M H}_2\text{SO}_4$ containing $5 \times 10^{-5}\text{ M}$ of: \times Ephedrine, \bullet Harmaline, \blacktriangle Cinchonine, \circ Codeine, \square Quinine

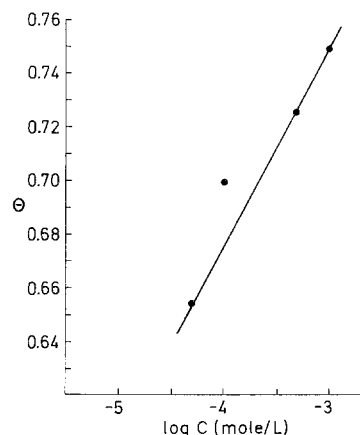


Fig. 4. The dependence of the degree of coverage of the iron surface with brucine on its concentration in $2\text{ M H}_2\text{SO}_4$

interaction with the metal surface. Retardation of iron dissolution by the additives of this study is expected to be due to their adsorption on the metal surface *via* the oxygen and nitrogen atoms. Brucine is found to be the most efficient inhibitor. This may be due to the presence of three centers of adsorption (two oxygen and one nitrogen atoms). Quinine has also three centers of adsorption (two oxygen and one nitrogen atoms), but is ranked after brucine. This is may be due to its lower molecular weight (size) with respect to brucine. Codeine comes after brucine and quinine, although it has three centers of adsorption (three oxygen atoms). This can be explained on the basis that the nitrogen atom is more basic than the oxygen atom and the inhibitor efficiency [8] should follow the sequence $\text{O} < \text{N} < \text{S}$.

Cinchonine, harmaline, and ephedrine each have two centers of adsorption (oxygen atom and nitrogen atom), but ephedrine ranks lower than after cinchonine and harmaline. This may be due to the difference in their molecular weights (sizes).

Table 3. Energy E^\ddagger , enthalpy change (ΔH^\ddagger), entropy change (ΔS^\ddagger), and free energy of activation change (ΔG^\ddagger) for iron dissolution in 2 M sulphuric acid in presence of 5×10^{-4} M of different inhibitors at different temperature (E^\ddagger , ΔH^\ddagger , ΔG^\ddagger : kcal·mol⁻¹; ΔS^\ddagger : cal·mol⁻¹·K⁻¹)

Temperature (K)	303	308	313	318	323
Brucine					
E^\ddagger			11.51		
ΔH^\ddagger	12.11	12.12	12.13	12.14	12.15
$-\Delta S^\ddagger$	25.15	26.30	27.35	28.24	30.68
ΔG^\ddagger	19.73	20.22	20.69	21.12	22.06
Quinine					
E^\ddagger			11.31		
ΔH^\ddagger	12.12	12.13	12.14	12.15	12.16
$-\Delta S^\ddagger$	19.42	21.19	21.90	23.06	24.23
ΔG^\ddagger	18.00	18.46	18.99	19.48	19.98
Codeine					
E^\ddagger			10.75		
ΔH^\ddagger	11.36	11.37	11.38	11.39	11.40
$-\Delta S^\ddagger$	22.39	23.97	24.65	26.03	26.67
ΔG^\ddagger	18.14	18.75	19.09	19.98	20.01
Cinchonine					
E^\ddagger			9.21		
ΔH^\ddagger	9.82	9.83	9.84	9.85	9.86
$-\Delta S^\ddagger$	28.07	29.30	29.89	30.80	31.62
ΔG^\ddagger	18.32	18.85	19.19	19.64	20.07
Harmaline					
E^\ddagger			7.37		
ΔH^\ddagger	7.98	7.99	8.00	8.01	8.02
$-\Delta S^\ddagger$	34.47	35.53	36.05	36.77	37.47
ΔG^\ddagger	18.42	18.93	19.28	19.70	20.12
Ephedrine					
E^\ddagger			7.09		
ΔH^\ddagger	7.70	7.71	7.72	7.73	7.74
$-\Delta S^\ddagger$	35.49	36.64	37.14	37.84	38.53
ΔG^\ddagger	18.45	18.99	19.34	19.76	20.18
2 M Sulphuric acid					
E^\ddagger			6.82		
ΔH^\ddagger	7.43	7.44	7.45	7.46	7.47
$-\Delta S^\ddagger$	36.48	36.64	38.35	38.91	39.64
ΔG^\ddagger	18.48	18.72	19.45	19.83	20.27

The inhibiting action of these compounds is also assumed to be an outcome of the cationic species resulting from the protonization of the N atom. The presence of the sulphate has been proposed to facilitate the adsorption of organic cations, due to the fact that they form intermediate bridges in which the negative ends of the sulphate metal dipoles may be oriented towards the solution. The formation of these dipoles will, therefore, increase with the increase of sulphate concentration.

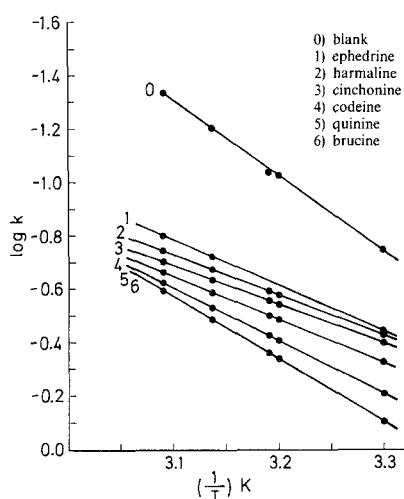


Fig. 5. Arrhenius plot of the corrosion rate of iron in 2 M H_2SO_4 in absence and presence of inhibitors

The effect of temperature on the dissolution of iron in the presence and in the absence of additives has been studied by the polarization technique. The corrosion rates were also determined at 30 °C, 35 °C, 40 °C, 45 °C, and 50 °C in the presence of 5×10^{-4} M inhibitor. From the previous experimental findings it is evident that the corrosion rate increases with increasing temperature, a result which is in accordance with the Arrhenius law in the temperature range used (Fig. 5). The plots are rectilinear and the activation energies are calculated from the slope of the curves. The Arrhenius activation energy values, obtained from the slopes of $\log k$ vs. $1/T$ are presented in Table 3. These values increase with increasing inhibition efficiency of the additives and suggest that the process is controlled by the surface reaction, since the energy of activation for the corrosion process is above 5 kcal [11].

The values of free energy of adsorption G_{ads}° are given in Table 3 at different temperatures. The results show that brucine, which gives maximum efficiency, shows a higher activation energy of the iron dissolution reaction. The free energy of activation increases with increasing temperature in absence and in presence of additives.

Experimental

Iron test samples containing 0.06% C, 0.005% P, 0.25% Mn, 0.019% S, 0.04% Si, 0.05% Cr, 0.035% Ni, 0.07% Cu, and 99.47% Fe were used; all chemicals were a.r. quality. The solution of 2 M sulphuric acid was prepared with twice-distilled water.

For the galvanostatic studies, circular 0.53 mm diameter wire samples were cut, the actual area exposed through a teflon window being 0.22 cm². Before immersion, the samples were polished with 500 emery paper and degreased. The solution in the electrolytic cell had a volume of 100 cm³. For the potential measurements, those described by Gatos were employed [7]. All potentials were measured with respect to a saturated calomel electrode (SCE). The inhibitive efficiency was calculated from the formula

$$\% \text{ Inhibition} = (1 - i_1/i_0) \times 100 \quad 1$$

where i_1 and i_0 are the corrosion currents with and without inhibitor, respectively.

The thermodynamic function $E^\#$ (Arrhenius energy of activation), $\Delta G^\#$ (free energy of activation), $\Delta H^\#$ (enthalpy of activation), and $\Delta S^\#$ (entropy of activation) were calculated from the following equations:

$$\log k = (E^\#/2.303RT) + \text{const.} \quad 2$$

$$H^\# = E^\# + RT \quad 3$$

$$\Delta G^\# = RT(\ln kT/h - \ln k) \quad 4$$

$$\Delta S^\# = (\Delta H^\# - \Delta G^\#)/T \quad 5$$

(R = gas constant, T = absolute temperature, h = *Planks* constant, k = *Boltzmann* constant, k = rate constant).

References

- [1] Schmitt G., Bedbur K. (1984) Proc. 9th Int. Congr. Met. Corros. Toronto, Canada, p 112
- [2] Granese, S. L., Rosales, B. M., de Gonzalez C. O. (1989) Proc. 3rd Iberoamerican Congr. Corrosion and Protection, Rio de Janeiro, Brazil, p 1049
- [3] Granese S. L. (1987) Proc. 10th Int. Congr. Met. Corrosion, Madras, India, p 2733
- [4] Granese S. L., de Gonzalez, C. O., Rosales B. M. (1988) *Quimindustria*'88, La Habana Cuba, p 176
- [5] Granese S. L. (1985) Proc. 6th European Symp. Corrosion Inhibitors, Ferrara Italy, p 227
- [6] Granese S. L. (1988) *Corrosion* **44**: 322
- [7] Gatos H. S. (1956) *Corrosion* **12**: 23
- [8] Donnelly B., Downie T. C., Grzeskowiak R., Hamburg, H. R., Short D. (1974) *Corros. Sci.* **14**: 597
- [9] Conway B. E. (1965) *Theory and principles of electrode processes*. The Ronald Press, New York, p 81
- [10] Khitrov V. A. (1960) *Izv Voronezhsk, Gos. Ped. Inst.* **29**: 5
- [11] Fouda A. S., Elasklany A. H., Madkour L. H. (1984) *Indian J. Chem. Soc.* **61**: 425

Received December 3, 1993. Accepted September 26, 1994